STAFF SUMMARY SHEET

	TO	ACTION	SIGNATURE (Surname), GRADE AND DATE		TO	ACTION	SIGNATURE (Surname), GRADE AND DATE
1	DFAN	sig	James k Hall	6			
2	DFER	approve	Kraus, Col 13 Jun 13	7			Standardize commas or periods as decimal places and thousand separators
3	DFAN	action	(Author /Originator)	8			
4				9			
5				10			

SURNAME OF ACTION OFFICER AND GRADE	SYMBOL	PHONE	TYPIST'S INITIALS	SUSPENSE DATE
Thomas E. McLaughlin	DFAN	333-2613	rmc	20130624

SUBJECT: Clearance for Material for Public Release — USAFA-DF-PA- 384 — DATE:

SUMMARY

1. PURPOSE. To provide security and policy review on the document at Tab 1 prior to release to the public.

2. BACKGROUND.
Authors: Brice Aghababian, Benoit Reymond, and Russell M. Cummings

Title: Numerical Simulation of the Nozzle and Test Section of a Mach 6 Ludwieg Tube

Circle one: Abstract Tech Report Journal Article Speech (Paper) Presentation Poster

Thesis/Dissertation Book Other: _____

Check all that apply (For Communications Purposes):

[] CRADA (Cooperative Research and Development Agreement) exists

[] Photo/ Video Opportunities [] STEM-outreach Related [] New Invention/ Discovery/ Patent

Description: This is a paper describing the flow description for our Mach 6 Ludwieg Tube facility.

Release Information:

Previous Clearance information: (If applicable) None

Recommended Distribution Statement: Distribution A: approved for public release, distribution unlimited

3. DISCUSSION.
The paper will be presented at the AIAA Fluid Dynamics Conference in San Diego, CA. The first two authors were French Air Force Academy summer students in 2012.

4. RECOMMENDATION.

/signature/
(signature)
Thomas E. McLaughlin, PhD, DFAN
Professor

Numerical Simulation of the Nozzle and Test Section of a Mach 6 Ludwieg Tube

Brice Aghababian[1] and Benoit Reymond[2]
Ecoles d'officiers de l'Armée de l'air, Salon Air, 13661, France

Russell M. Cummings[3]
United States Air Force Academy, USAF Academy, CO, 80840, USA

In preparation for the arrival of a Mach 6 Ludwieg Tube at the United States Air Force Academy, a numerical simulation of the flow field within the test section of the wind tunnel has been undertaken. The goal of the project was to evaluate and numerically simulate the Mach 6 flow within the test section of the wind tunnel. These calculations allow for the determination of the size and conditions of the usable area within the test section. Relationships between the local Mach number and the position of a model in the test section were established, and flow parameters at the observation windows were studied, which will be used to position a Background-Oriented Schlieren system in the tunnel. The results will aid in future simulations of the Ludwieg Tube wind tunnel, and for comparisons with experimental results from the Mach 6 Ludwieg Tube wind tunnel after it is installed, as well as with results from similar Ludwieg Tubes at other institutions.

I. Introduction

THE United States Air Force Academy (USAFA) has an Aeronautics Research Center (ARC) which contains a wide variety of experimental facilities. The wind tunnels in the center include numerous subsonic and supersonic wind tunnels which are used for research and education, all involving faculty and cadets in important "real world" investigations. However, the ARC is not equipped with a wind tunnel that reaches Mach 6, and so the study of hypersonic flow has not been possible. This experimental gap will be filled late in 2012 with the addition of a Ludwieg Tube capable of hypersonic speeds being developed by the German company *Hyperschall und Strömungstechnick Gmbh* (HST). This new facility will help to complete the wind tunnel speed regimes available at USAFA, and will permit the researchers at ARC to reach hypersonic conditions for the first time. Indeed, only eighteen Ludwieg tubes are known to be operational in the world, making the USAFA tunnel important for future hypersonic investigations.[1]

A Ludwieg Tube is an alternative to traditional, expensive ground-based experimental facilities for hypersonic flow. Because of their low operational cost and good flow quality, Ludwieg tube blow-down tunnels are of special interest for hypersonic testing. Ludwieg tubes do not require a total pressure control device or large settling chamber which are common for conventional blow-down tunnels (such as the Trisonic Wind Tunnel, TWT, at the US Air Force Academy, USAFA). This greatly reduces the size and cost of operating the tunnel, since large compressors, heaters, and pressure vessels are not required for their operation. The operational costs for a Ludwieg tube have been further reduced by the use of a fast-acting valve instead of the traditional bursting diaphragm that was originally part of the tunnel design in the 1950s in Germany.[2]

Since no mechanisms are necessary to control pressure or temperature during the run of a Ludwieg tube, the tunnel can be described as an 'intelligent' blow down facility.[3] The following is a description of how the Ludwieg tube works, as highlighted in Fig. 1. The test gas, which is typically air, nitrogen, or helium, is stored in a long charge tube. The charge tube is connected to the nozzle, test section, and vacuum tank via a fast-acting valve. Once the valve is opened, an unsteady expansion wave travels at the speed of sound, a_T, down the charge tube. This expansion wave accelerates the gas to a tube Mach number, Ma_T, which is determined by the area ratio of the tube

[1] Officer Cadet, currently Lieutenant, French Air Force.
[2] Officer Cadet, currently Lieutenant, Escadron de Chasse 2/4 "La Fayette", French Air Force.
[3] Professor of Aeronautics, Department of Aeronautics, AIAA Associate Fellow.

and the nozzle throat. The expansion wave travels up and down the tube, which creates a constant steady flow to the expansion nozzle with pressure and temperature determined by the one-dimensional unsteady expansion process. Upon the return of the reflected wave from the end of the tube to the nozzle throat, the valve is closed and the test run is completed. The length of the tube, L, and the speed of sound in the tube, a_T, determines the run time, t_R, of the tunnel.[3]

When compared to a standard blow-down tunnel, the Ludwieg tube provides the following advantages.[3,4]

- an extremely short start and shut off time for the tunnel
- no regulation of pressure and temperature during the run time is necessary
- extremely low mass and energy loss during the tunnel start and shut off
- due to the elimination of regulation valves, the entrance flow to the nozzle can be kept extremely clean, which results in flow with low turbulence levels
- a facility very well suited for transient heat transfer tests
- the tunnel has no "unit Reynolds number" effects like other tunnels
- from the first three advantages listed above you obtain *an extremely affordable test facility*, requiring only typical laboratory power for operation

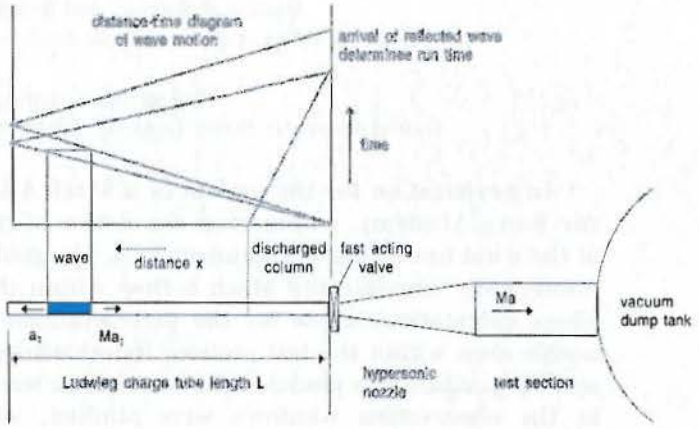

Figure 1: Hypersonic Ludwieg Tube operating principle with wave diagram.[3]

The Mach number in the test section is determined by the nozzle and corresponding throat inserts. The stagnation pressure and temperature can be adjusted from the main control board prior to a shot. The interval between shots can be as low as four minutes (due to the relatively small volume of air in the charge tube), and the shot duration is approximately 100*ms*. The short duration of the shot is the only real disadvantage of the tunnel, requiring high-speed measurement and control equipment to make meaningful measurements of the flow field.

The specific layout and design of the USAFA Ludwieg Tube is shown in Fig. 2. The tube will have a 0.5m diameter test section and an insulated charge tube of 27m in length, which will produce a run time of approximately 100ms and a shot time of ~10 minutes. The test gas (in this case air) will be heated, dried, and compressed until it reaches approximately 670 K and 40 bars in the tube. This design will allow the tube to be used for both transition testing on cones and blunt bodies, as well as heat transfer testing on blunt bodies. A fast-acting valve is located at the end of the charge tube which opens into a nozzle designed to create uniform Mach 6 flow in the test section. A straight diffuser section precedes the $6m^3$ vacuum tank, which will be required to maintain 1 mbar of pressure after the run. The overall length of the Ludwieg tube is approximately 35m. Several of the sub-components of the Ludwieg tube will be described below, including details of their capability and equipment requirements. Most of this information is based on the design work of HST, included in their design document.[5] The run test lasts for approximately 100 milliseconds (ms), and the system requires about 6 minutes to be ready to test again.

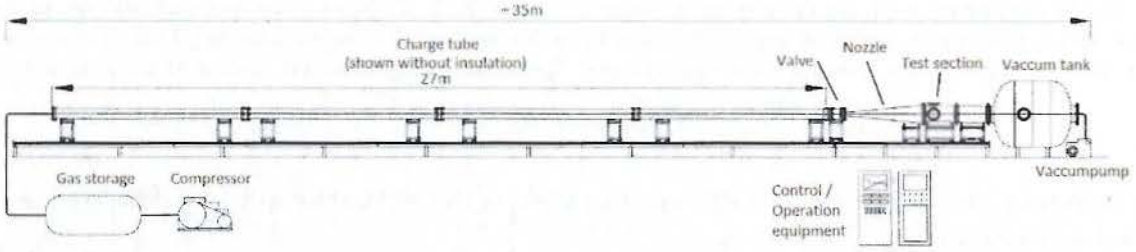

Figure 2: Design layout of USAFA Ludwieg tube

Computational Fluid Dynamics (CFD) will be used to simulate the flow from the valve through the test section of the Ludwieg Tube shown in Fig. 2. The results of a grid resolution study will be presented, and the conditions leading to Mach 6 flow in the test section will be evaluated. In addition, evaluation of the condensation limits of the tunnel will be presented in later sections.

II. Computational Methodology

Since the CFD simulations will include subsonic through hypersonic flow, a compressible flow solver is required. In our case, traditional solvers like small disturbance velocity potential or even full potential may not be adequate, so either Navier-Stokes or Euler equations should be used. In addition to the appropriate flow solver, we used a computer cluster at the USAFA Modeling & Simulation Research Center (MSRC). This computer cluster is an SGI Altix Ice which runs 144 Cores, with 2 GB Memory per core. The simulations used 60 cores to run our calculations and each simulation took around 30 minutes to be completed. The software used in the study included GridGen for mesh generation, Cobalt for flow solutions, and FieldView for flow visualization. Each of these will be discussed in the next sections.

A. Equations of Fluid Motion and Flow Solver

In our study we will simulate a hypersonic wind tunnel, so it was important to use the right choice in equation sets. Most flow solvers today include the Navier-Stokes equations (coupled with the Perfect Gas Law and Sutherland's Law) to define fluid flow. In our case we will consider our fluid as inviscid and we will use the Euler equations, which are simplified from the Navier-Stokes equations by assuming that the flow is inviscid. The Euler equations are based on the conservation of mass, momentum, and energy, and can be applied to compressible flow at a variety of Mach numbers.

The flow solver used for our study is the Cobalt flow solver by Cobalt Solutions LLC[6] that solves the unsteady, three-dimensional and compressible Navier-Stokes equations in an inertial reference frame. These equations in integral form are:

$$\frac{\partial}{\partial t}\iiint \bar{Q}d\forall + \iint \left(\vec{f}\hat{i} + \vec{g}\hat{j} + \vec{h}\hat{k}\right)\cdot \hat{n}dS = \iint \left(\vec{r}\hat{i} + \vec{s}\hat{j} + \vec{t}\hat{k}\right)\cdot \hat{n}dS$$

where $\forall$ is the fluid element volume; S is the fluid element surface area; $\hat{n}$ is the unit normal to S; $\hat{i}$, $\hat{j}$, and $\hat{k}$ are the Cartesian unit vectors; $\bar{Q} = \left(\rho, \rho u, \rho v, \rho w, \rho e\right)^T$ is the vector of conserved variables, where ρ represents the air density, u, v, and w are velocity components and e is the specific energy per unit volume. The vectors $\vec{f}$, $\vec{g}$, and $\vec{h}$ represent the inviscid components, the superscript T denotes the transpose operation, and the vectors $\vec{r}$, $\vec{s}$, and $\vec{t}$ represent the viscous components.

Cobalt solves the unsteady, three-dimensional, compressible Navier-Stokes equations. Cobalt is a cell-centered, finite volume based code applicable to arbitrary cell topologies including prisms, tetrahedra, and hexahedrals. Second-order accuracy in space is achieved using the exact Riemann solver of Gottlieb and Groth,[7] and least squares gradient calculations using QR factorization. To advance the discretized system a point-implicit method using analytic first-order inviscid and viscous Jacobians is used. A Newton sub-iteration method is used in the solution of the system of equations to improve time accuracy of the point-implicit method. The method is second-order accurate in time. Tomaro et al.[8] converted the code from explicit to implicit, enabling CFL numbers as high as 10^6.

The Cobalt solver calculates velocity in the three directions (X, Y, Z), density and pressure, and we needed to know speed, temperature, speed of sound, Mach and Reynolds number all along the Ludwieg Tube. These variables were defined in FieldView using the following relations. The velocity magnitude was calculated using the formula:

$$|V| = \sqrt{u^2 + v^2 + w^2}$$

For temperature, the ideal gas law $pv = RT$ was used, where we then replaced the specific volume with $v = 1/\rho$, to find the temperature as:

$$T = \frac{p}{\rho R}$$

The Mach number depends on speed and temperature, so we used the following relation to define the Mach number:

$$M \equiv \frac{|V|}{a} = \frac{\sqrt{u^2 + v^2 + w^2}}{\sqrt{\gamma RT}}$$

Finally it was necessary to calculate the Reynolds number, which required calculating the molecular viscosity with Sutherland's formula:

$$\mu = C_1 \frac{T^{3/2}}{T + C_2}$$

where $C_1 = 1.458 \times 10^{-6}\ \mathrm{N \cdot s/(m^2 \cdot K^{1/2})}$ and $C_2 = 110.4\ K$. The unit Reynolds number (Reynolds number per meter) is then defined as:

$$\frac{\mathrm{Re}}{L} = \frac{\rho |V|}{\mu}$$

B. Computational Mesh

The choice of an appropriate mesh is essential to the proper simulation of any flow. To insure the best results, three different grids were created to run simulations. The mesh was started with a CAD file which had been obtained from the Ludwieg Tube manufacturer in Germany, and then a mesh was created with GridGen. The CAD file defines the Ludwieg Tube interior surface then a surface mesh was created. In order to create meshes with different numbers of cells, the number of cells on the surface were adjusted to three different levels. Our mesh represents a 4.38 meter-long portion of the Ludwieg Tube, which is really composed of four different parts, as shows Figure 3. Included in the simulation are the fast-acting valve (shown in blue), the nozzle (shown in green), the test section (shown in yellow), and the diffuser (shown in red). These sections provided a good simulation of the important aspects of the flow through the test section.

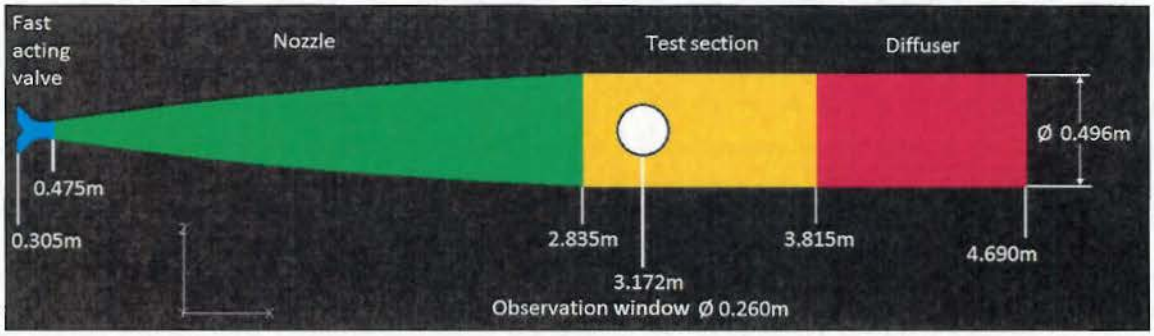

Figure 3: Actual grid composition, notice the position of the window which allows direct observation of a model in the flow

A grid consists of millions of cells, which delimit boundaries, and can have many faces formed by different shapes, such as triangles, hexahedra, or polygons. A representative view of the mesh is shown in Fig. 4, where close-ups of the mesh in different regions is shown.

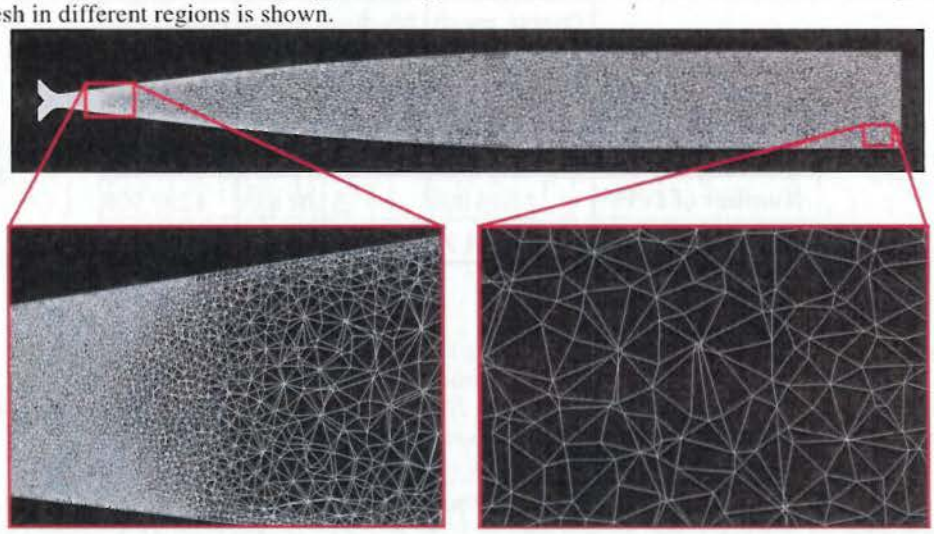

Figure 4: 2D view in plane (0;X;Z) of the medium Ludwieg Tube grid, with two different portions shown in detail.

For each cell, values of pressure, temperature, and other parameters are calculated during the simulation to establish a continuous flow field for each value. Face size are not constant, because a large number of small cells are required where parameters change a lot, in a short time and in a short distance. Figure 5 shows the mesh close to the Ludwieg Tube throat, where we need a high accuracy because parameters fluctuate a great deal.

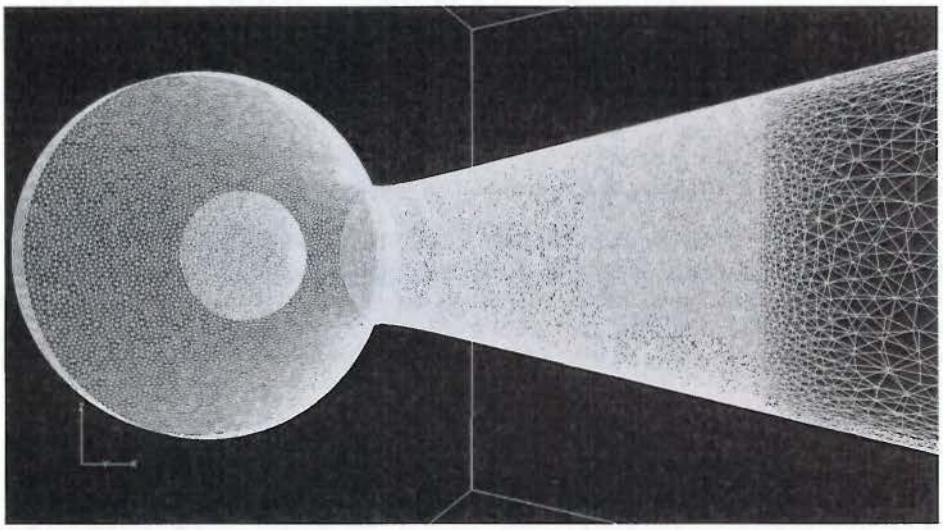

Figure 5: 3D view of the grid in the vicinity of the throat.

To determine the quality of a grid we need to focus on a grid sensitivity study using the three meshes generated: coarse, medium, and fine. Table 1 compares the sizes and estimated quality (determined by Cobalt) of the three different meshes. Notice that the grid using the fine mesh has the best mesh quality and also the highest number of points, faces and cells, but a sensitivity study will show if the extra cells are required for this simulation.

Table 1 : Grids parameters and quality rate calculated by Cobalt.

	Coarse mesh	Medium mesh	Fine mesh
Number of zones	60	60	60
Number of points	325 439	690 182	831 706
Number of Faces	3 186 388	7 226 828	8 810 141
Number of Cells	1 525 869	3 508 633	4 287 909
Quality	94,77	95,62	95,71

We performed the grid sensitivity study by evaluating the pressure at one point in the test section: (X=2.8; Y=0; Z=0), which is a point on the centerline of the test section corresponding to the beginning of the test zone. To determine pressures at this location we created a .tap file which Cobalt uses to save pressure values for each iteration. Results from the .tap file for each mesh are shown during the simulation in Fig. 6.

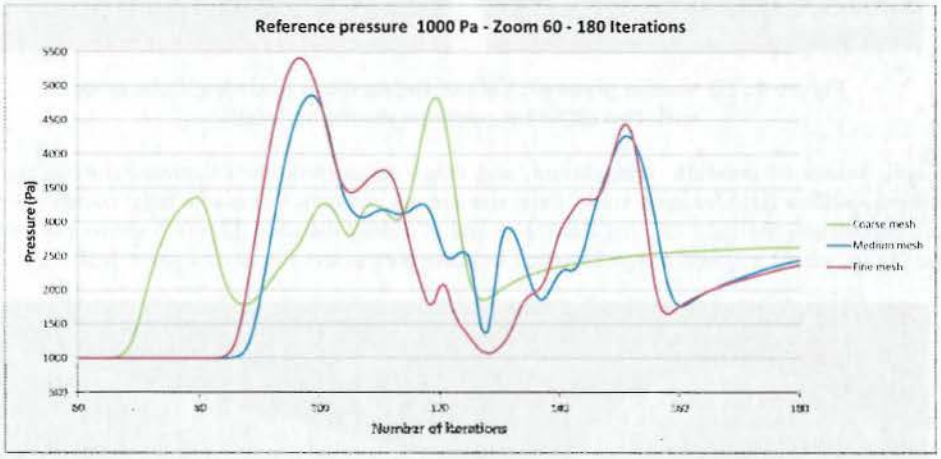

Figure 6: Pressure as a function of iterations at location (2.8 ; 0 ; 0).

We noticed that the three meshes seem to give similar overall results, with a 0,63% difference between the three meshes. Figure 7 shows the simulations at the end of each run (the fine mesh takes longer to converge than the other meshes), where it is apparent that the red and the blue curves are very similar, which means that the medium mesh is as accurate as the fine mesh. Since the fine mesh takes a longer time to converge (29,57 seconds) than the medium mesh (4,67 seconds), the medium mesh was used for all further simulations.

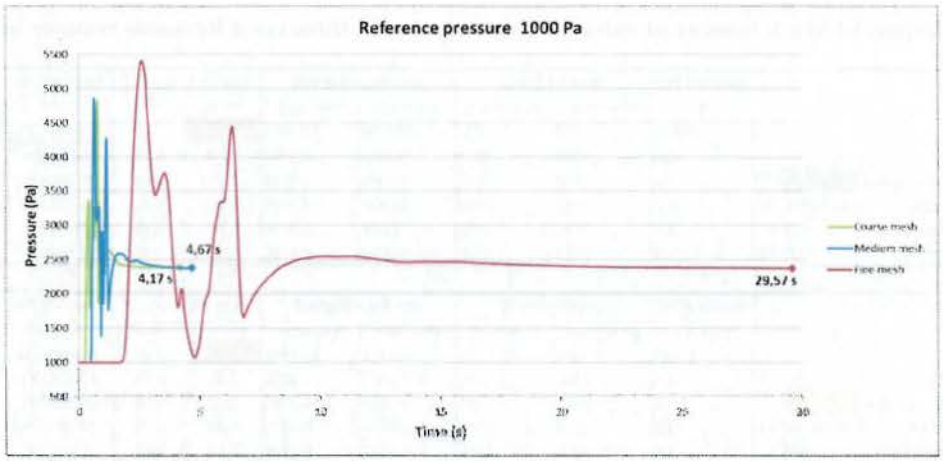

Figure 7: Pressure as a function of time at (2.8 ; 0 ; 0).

C. Boundary Conditions

To run calculations on Cobalt, we need to define the various boundary conditions. The boundary conditions enables us to change the tunnel inflow and outflow parameters, which are especially important for these internal flow simulations. For inflow we can modify static pressure, static temperature, omega, or Mach number. These parameters define Riemann Invariants which enables us to apply specific values to simulate hypersonic flow. We used floating values for other conditions so we do not over-define the boundary conditions at these locations. We also chose a static outflow pressure. On the solid surfaces we used the slip boundary condition for inviscid flow.

In our initial simulations we varied some of these parameters in order to determine the sensitivity of the solution to the boundary conditions (see Table 2). We varied inflow Mach, from 0.0 to 1.0 in order to have Mach 1 at the throat and Mach 6 flow in the test section. We also modified static pressure and temperature to determine simulation limits. We found ten combinations of variables that create a Mach number at the exit valve which provides Mach 1 at the throat. We concluded that the shape of the nozzle offers correct flow conditions for a large number of conditions, which is a testament to the quality of the design of the tunnel. The various portions of Table 2 contain:

- Column 1: the charge pressure, charge temperature, the Mach number at valve, and the outflow pressure are settings before calculations
- Column 2: X is the reference distance of mesh, from valve is the real distance from the closed valve
- Column 3 and 5: the pressure and density are given by Cobalt results
- Column 4, 6, 7, 8 and 9: speed, temperature, Mach number, viscosity and Reynolds number come from the equations developed earlier

Table 2 : Impact of Mach number at valve on Mach number at throat and Reynolds number in test section

		Position (m)	Speed S (m/s)		Density ρ (kg/m3)		Mach = S/√(γ.r.T)		Reynolds Re/L (1/m) = ρ.S/μ	
		X	minimum	maximum	minimum	maximum	section	centre	section	centre
		0,415	419	522	10,7368	13,3117	1,01	0,89	201 797 735	194 667 650
		2,8	1052	1072	0,1012	0,1344	5,64	5,53	20 604 626	16 856 533
Mach number at valve	0	3	1052	1075	0,0945	0,1353	5,73	5,62	20 782 522	16 219 618
charge pressure	4 000 000 Pa	3,2	1052	1076	0,0882	0,1259	5,86	5,76	20 270 416	15 898 354
charge temperature	673 K	3,4	1052	1077	0,0824	0,1206	5,95	5,86	19 850 362	15 415 302
outflow pressure	1000 Pa	3,6	1053	1076	0,0772	0,1166	5,99	5,88	19 267 689	14 553 811

		Position (m)	Speed S (m/s)		Density ρ (kg/m3)		Mach = S/√(γ.r.T)		Reynolds Re/L (1/m) = ρ.S/μ	
		X	minimum	maximum	minimum	maximum	section	centre	section	centre
		0,415	461	576	20,8111	25,8991	1,01	0,89	381 145 131	368 309 992
		2,8	1160	1180	0,1977	0,2600	5,65	5,53	36 304 379	29 781 849
Mach number at valve	0,5	3	1161	1182	0,1831	0,2587	5,72	5,58	35 792 725	28 046 715
charge pressure	4 000 000 Pa	3,2	1164	1185	0,1703	0,2401	5,85	5,72	34 736 978	27 318 822
charge temperature	673 K	3,4	1165	1187	0,1587	0,2294	5,93	5,82	33 765 988	26 291 391
outflow pressure	1000 Pa	3,6	1168	1189	0,1490	0,2227	5,99	5,86	32 995 506	25 001 201

		Position (m)	Speed S (m/s)		Density ρ (kg/m3)		Mach = S/√(γ.r.T)		Reynolds Re/L (1/m) = ρ.S/μ	
		X	minimum	maximum	minimum	maximum	section	centre	section	centre
		0,415	493	620	31,0473	38,3385	1,01	0,88	554 321 788	530 699 056
		2,8	1242	1268	0,2940	0,3888	5,65	5,54	50 456 264	41 480 350
Mach number at valve	0,9	3	1243	1271	0,2728	0,3878	5,72	5,61	50 041 288	39 297 633
charge pressure	4 000 000 Pa	3,2	1246	1273	0,2533	0,3592	5,84	5,73	48 189 356	38 000 811
charge temperature	673 K	3,4	1248	1276	0,2364	0,3423	5,93	5,83	46 823 048	36 552 446
outflow pressure	1000 Pa	3,6	1250	1278	0,2201	0,3324	5,98	5,87	45 463 482	34 522 155

III. Results and Discussion

To accurately complete the computational modeling of the Ludwieg Tube, we had to compare results from three series of calculations. In each simulation we will note values at specific locations in the test section, as shown in Fig. 8. The first comparisons were made to determine the inflow boundary conditions, which was already discussed. The second series of comparisons were made to determine the influence of the vacuum tank pressure (outflow) on the results. We performed three different simulations with an outflow pressure at 50 Pa (pump characteristic), 1000 Pa (the lowest pressure which permit us to finish all calculations) and 101,300 Pa (atmospheric pressure). With an outflow pressure under 1000 Pa the simulations did not converge. The overall results are related in Table 3, where we can see that the outflow pressure (other than for cases below 1000 Pa) does not influence the pressure, density, and speed throughout the nozzle and test section. This was satisfying, since the vacuum tank pressure determines if the tunnel will start, not the properties in test section, so this was a good verification of that fact.

or did you use Patm @ USAFA? (h=7k ft)

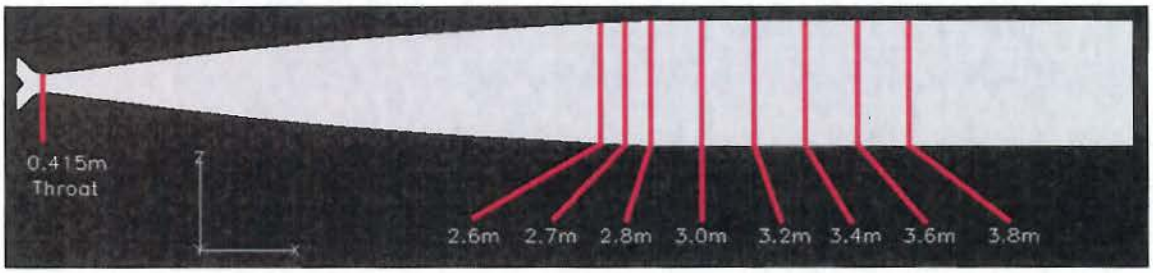

Figure 8: Different cutting planes used to compare values from simulations

Table 3 : Impact of outflow pressure throughout the wind tunnel

			Position (m)		Pressure p (Pa)		Speed S (m/s)		Density ρ (kg/m3)	
			X	*from valve*	minimum	maximum	minimum	maximum	minimum	maximum
			0,415	col	4 978 096	6 663 450	480	598	25,7739	31,4788
			2,8	2,494529	7 393	11 215	1208	1239	0,2392	0,3214
Mach number at valve	0,7		3	2,694529	6 603	11 004	1209	1242	0,2228	0,3186
charge pressure	4 000 000	Pa	3,2	2,894529	5 932	9 781	1212	1244	0,2074	0,2966
charge temperature	673	K	3,4	3,094529	5 418	9 075	1214	1247	0,1922	0,2831
outflow pressure	50	Pa	3,6	3,294529	4 922	8 696	1216	1250	0,1785	0,2737

			Position (m)		Pressure p (Pa)		Speed S (m/s)		Density ρ (kg/m3)	
			X	*from valve*	minimum	maximum	minimum	maximum	minimum	maximum
			0,415	col	4 973 703	6 659 831	481	598	25,7493	31,4077
			2,8	2,494529	7 387	11 253	1208	1237	0,2398	0,3222
Mach number at valve	0,7		3	2,694529	6 605	11 051	1209	1240	0,2232	0,3186
charge pressure	4 000 000	Pa	3,2	2,894529	5 936	9 788	1212	1243	0,2082	0,2968
charge temperature	673	K	3,4	3,094529	5 418	9 072	1214	1246	0,1930	0,2832
outflow pressure	1000	Pa	3,6	3,294529	4 923	8 705	1216	1248	0,1793	0,2736

			Position (m)		Pressure p (Pa)		Speed S (m/s)		Density ρ (kg/m3)	
			X	*from valve*	minimum	maximum	minimum	maximum	minimum	maximum
			0,415	col	4 973 259	6 666 062	481	598	25,7481	31,4732
			2,8	2,494529	7 381	11 154	1208	1236	0,2393	0,3199
Mach number at valve	0,7		3	2,694529	6 608	11 036	1209	1240	0,2230	0,3187
charge pressure	4 000 000	Pa	3,2	2,894529	5 937	9 786	1212	1242	0,2079	0,2970
charge temperature	673	K	3,4	3,094529	5 427	9 070	1214	1245	0,1931	0,2830
outflow pressure	101300	Pa	3,6	3,294529	4 930	8 700	1216	1247	0,1797	0,2736

A. Test Section Parameters

In order to test a model in a wind tunnel, it is essential to obtain pressure and temperature conditions that give a desired Reynolds number and Mach number. Indeed, these non-dimensional numbers represents a flow regime, and and the fluid behavior. The Ludwieg Tube has a fixed Mach number (determined by the nozzle shape), but to obtain different Reynolds number in the test section it is necessary to adjust the pressure and temperature in the charge tube. Therefore, we have performed twenty calculations which gave us an operating range for the tunnel.

As describe above, using Mach 0 at the valve yielded 673 K and 40 bars. As a result, the Reynolds number is about 2.10^7 *1/m*, which is the value shown on Figure 9. In order to reduce the number of simulations, we decided to use the temperature limit given by the limitation of the heating tube – so the highest temperature is 673 K. The graph specifies a second limit named the *condensation limit*. This temperature is between 400 and 500 K.[5] The condensation limit will be studied in the next section, and as a first step we chose 400 K as the lowest temperature. In the same way as we have set the highest temperature, we have scaled the highest pressure at 40 bars; the lowest pressure chosen is 5 bars.

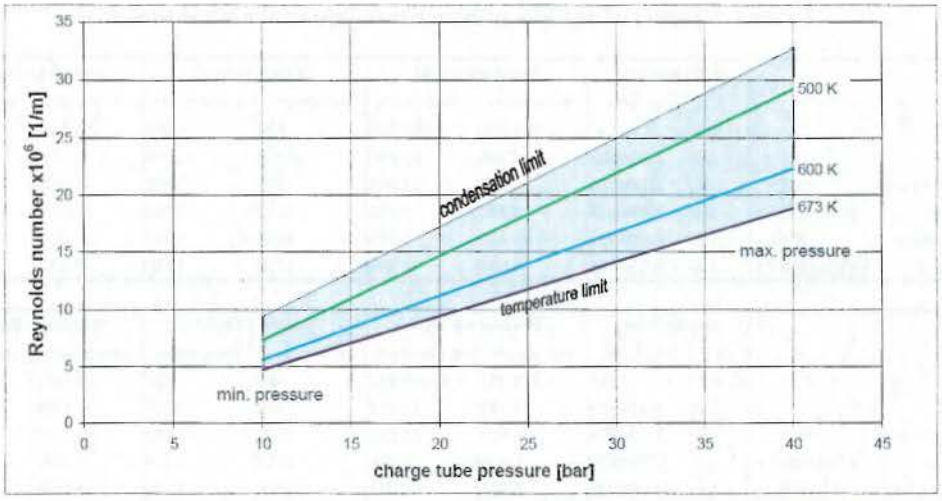

Figure 9: Maximum unit Reynolds number as a function of charge tube pressure and temperature.[5]

Figure 10 shows the Reynolds number as a function of charge tube pressure at X = 2,8 m and X = 3,6 m. Each color represents Reynolds numbers at a particular charge tube temperature, and between X = 2,8 m and X = 3,6 m. Both curves of each color describe a range of Reynolds numbers available for a given charge tube temperature; the values which appear on Fig. 10 are at the center of the test section. Here we can see that the Reynolds numbers, obtained with M = 0 inflow conditions, are close to the results shown by Fig. 9. Using the charge tube temperature T = 673 K, the Reynolds numbers range is from Re/L = 1,797,778 1/m to Re/L = 16,856,533 1/m. This gap is rather significant but lower temperatures offer greater ranges. At T = 400 K, the region starts at Re/L = 4,213,948 1/m and ends at Re/L = 38,814,684 1/m. At first sight, choosing a charge tube temperature T = 400 K seems to be more interesting for the use of this Ludwieg Tube. In addition, the fact that reducing this temperature would save energy and money, and increase the number of runs that could be performed.

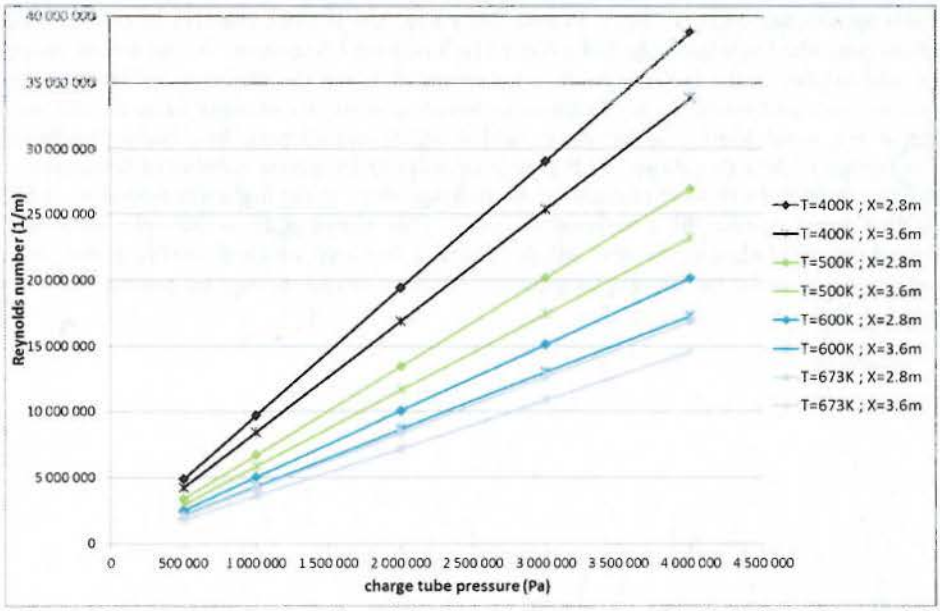

Figure 10: Reynolds number as a function of charge tube pressure at Y=Z=0, X = 2,8 m and X = 3,6 m.

B. Condensation

Condensation is a phenomenon where the test gas is changing into a solid form without ever having been a liquid. It happens for every chemical element at particular conditions of temperature and pressure. A Ludwieg Tube is able to reach Mach 6 due to the nozzle design, including the sonic throat, as shown in Fig. 11. With a normal throat, pressure and temperature decrease upstream, and increase downstream. So the speed reaches a maximum value at the throat. But with a sonic throat, the speed continues to increase in the nozzle and reaches supersonic and hypersonic speeds in the test section. This is the intended effect but it should be noted that the pressure and temperature are still decreasing throughout the divergent section. Because of these effects, the condensation conditions of each air chemical components can be reached in these tunnels.

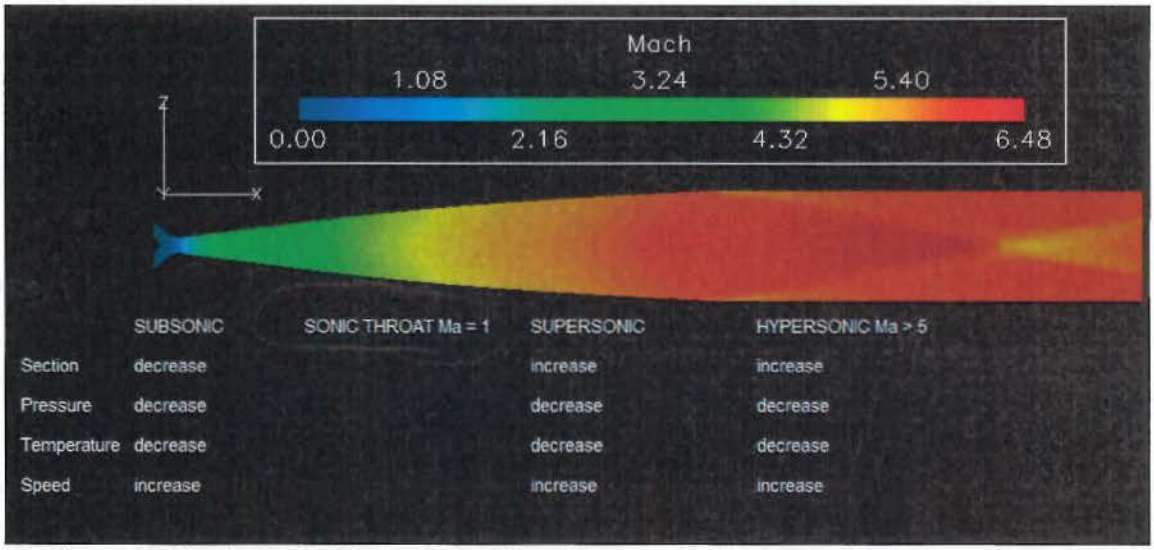

Figure 11: Physical quantities evolution throughout a convergent-sonic throat-divergent nozzle.

It is easy to understand that a solid object moving at Mach 6 would be dangerous for users, the wind tunnel and the model. Therefore, high speed tunnels are typically limited by condensation, which is why these limits are being evaluated here. The test gas which will be used in the USAFA Ludwieg Tube is dry air. This means that water is almost eradicated in the air by the use of a dryer prior to pressurization. "The absolute humidity in this air is $x_m = 5.82.10^{-5}$ which is far below chocking conditions. Even with extreme small absolute humidity levels of $x_m < 10^{-5}$ the H_2O partial pressure will pass the saturation condition at a Mach number of about Ma = 3."[5] However, the air stays compounded with other chemical elements during the test; most of this dry air is a compound of oxygen (21.0%) and nitrogen (78.1%). Saturation conditions of both of these are less stringent than air. But it continues to be necessary to observe their condensation and liquefaction limits, and in which cases these gases would change state. Our purpose here is to demonstrate that reducing the charge tube pressure and temperature can affect the measurements during a test.

First of all, we should observe the different saturation boundaries curves shown in Fig. 12, where we focus on oxygen, nitrogen, air, and water. The oxygen, nitrogen, and water curves are each compound with two parts separated by a point. Each point represents the triple point of each chemical element. A triple point is the combination of two values – temperature and pressure – where the three curves join. These curves are the gas-solid, gas-liquid and solid-liquid boundaries (solid-liquid boundaries are not representing here).

We will focus solely on the first two (gas-solid and gas-liquid) which seems to nearly form a single curve. On the right of this curve, the chemical element is a gas. On the left, it is solid on the down side of the triple point, and it is liquid on the top side of the triple point. We will demonstrate later the behaviors of the test gas throughout the nozzle and the test section.

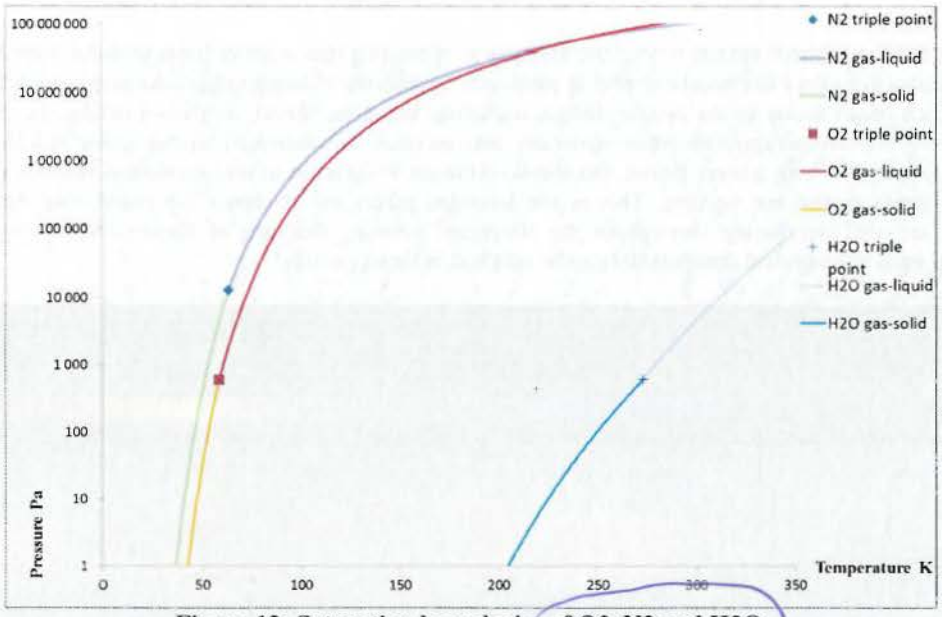

Figure 12: Saturation boundaries of O2, N2 and H2O.

Need Subscripts

To draw these curves, we must use the Rankine equations which give the saturation pressure relations for each element:

$$\log_{10} p = -\frac{A}{T} + B$$

Where A and B are constants for vapor pressure calculations given in Table 4.

Table 4: Constants for vapor pressure calculations.

	Constants for vapor pressure calculation logarithmic relation	
	A (K)	B (atm)
N2 g-s	359,1	4,778
N2 g-l	314,2	4,068
O2 g-s	437,5	5,25
O2 g-l	386	4,37
Air	336,3	4,114
H2O g-s	2676	7,582
H2O g-l	2263	6,064

We can then extract the pressure from:

$$p = 10^{B} 10^{-A/T}$$

Figures 13 through 16 represent the oxygen and nitrogen saturation boundaries, and the curves of dry air evolution characteristics with Mach number. Each figure represents results for a different charge tube temperature: Figure 13, charge tube temperature = 400 K. Figure 14, charge tube temperature = 500 K; Figure 15, charge tube temperature = 600 K; and Figure 16, charge tube temperature = 673.

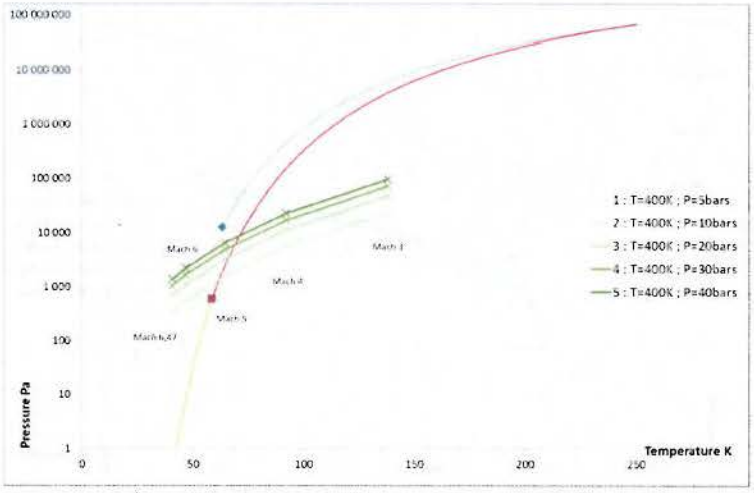

Figure 13: Test gas expansion with charge tube temperature T=400K, and saturation boundaries.

The first five simulations were conducted for a charge tube temperature at 400 K, and a charge tube pressure at 5, 10, 20, 30 and 40 bars. We can observe that curves number 2, 3, 4, and 5 cross the oxygen gas-liquid boundary around M = 5. Curve number 1 crosses the oxygen gas-solid boundary at the same Mach number. This means that at 5 bars oxygen crystalizes before reaching the test zone. At higher pressures oxygen becomes liquid and crystalizes between M = 5 and M = 6. Later in the tube, nitrogen crystalize before M = 6 for any charge tube pressure. This charge tube temperature is therefore too low for use in testing.

In the next case the charge tube temperature is 500 K, and the charge tube pressures are always 5, 10, 20, 30 and 40 bars. Curves 8, 9 and 10 show the same behavior of dry air at 400 K – first of all oxygen is liquefied then crystalized, and in a third situation nitrogen is crystalized. Curve 7 represents the dry air expansion at 10 bars, and now oxygen becomes solid and crosses the saturation boundary on the oxygen triple point. We can see now, at this charge tube pressure, nitrogen stay gaseous. This is exactly the same case with higher charge tube pressure, so with these conditions it is impossible to use the Ludwieg Tube without a risk.

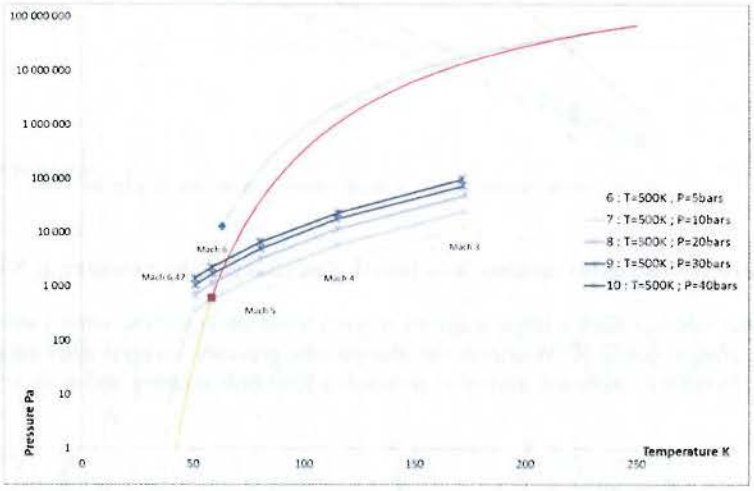

Figure 14: Test gas expansion with charge tube temperature T=500K, and saturation boundaries.

Figures 15 and 16 show results for 600 K as the charge tube temperature. The curves 11, 12 and 13 demonstrate that this temperature can be sufficient if the charge tube pressure does not exceed 20 bars. Indeed these three curves do not cross the saturation boundaries of oxygen and nitrogen. So it is possible to use this setting in order to realize run tests with models. But as we have seen in part Section 2.1, this choice can deprive users of reaching higher Reynolds numbers.[9] In addition, the compressors are able to pressurize up to 30 bars, so it is therefore possible to make a setting mistake and exceed 20 bars in the charge tube.

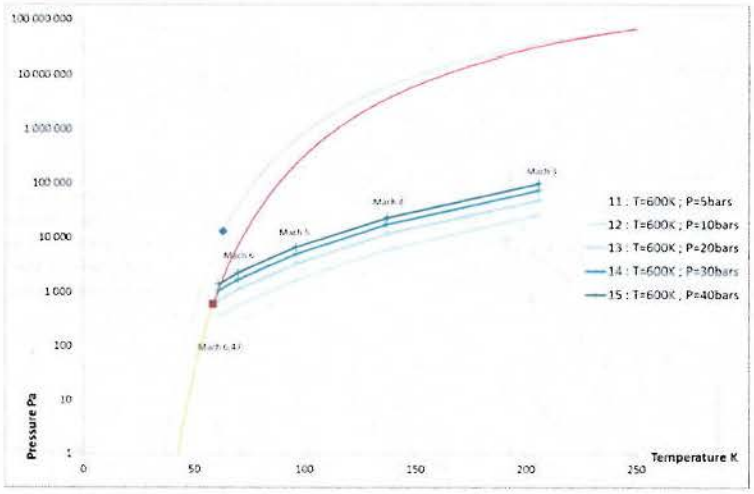

Figure 15: Test gas expansion with charge tube temperature T=600K, and saturation boundaries.

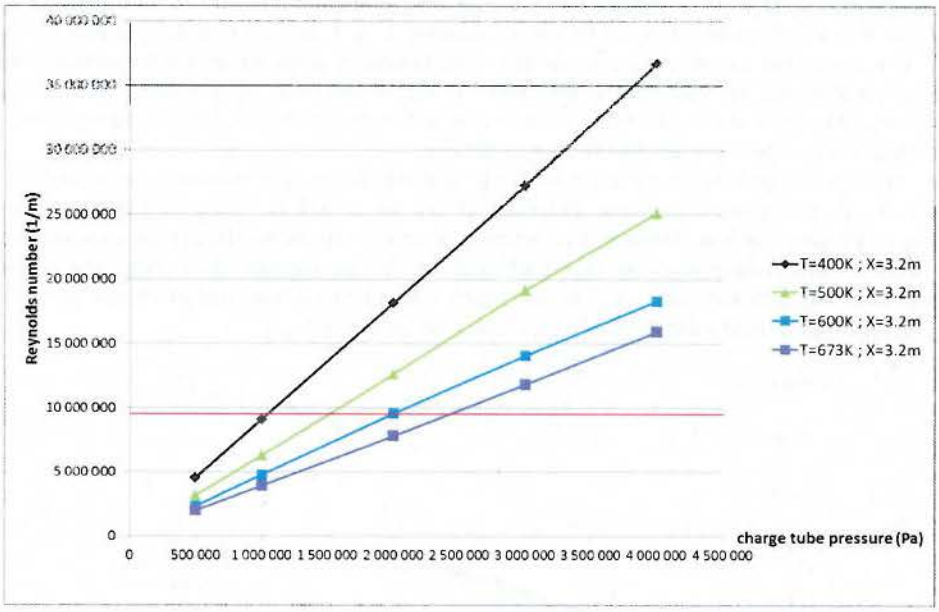

Figure 16: Reynolds number as a function of charge tube pressure at X=3.2m

The last case is that which offers a large range of Reynolds numbers for the wind tunnel (Figures 16 and 17). The charge tube temperature is 673 K. Whatever the charge tube pressure, oxygen and nitrogen do not change to a liquid or solid. In addition this conditions allows us to reach a Reynolds number above to $1.5X10^7$ 1/m in the entire test section.

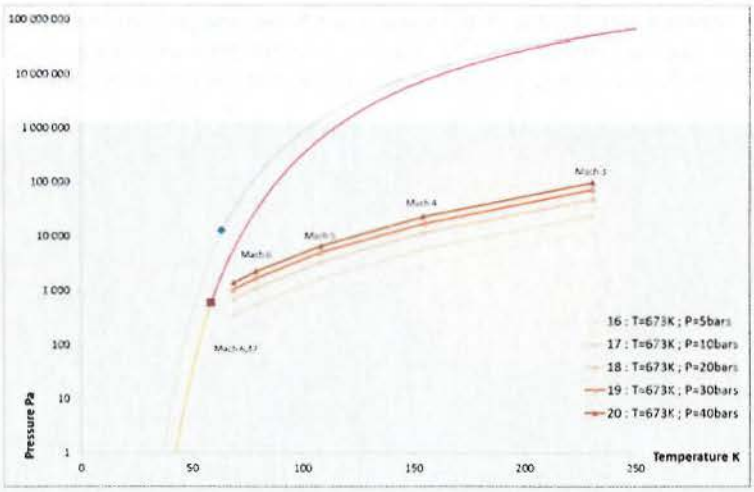

Figure 17: Test gas expansion with charge tube temperature T=673K, and saturation boundaries

Finally we observe that the condensation limit is more stringent than it appears when we study Fig. 9. A high temperature up to 600 K is necessary to obtain high Reynolds and not crystalize the gas. With lower temperature it is theoretically possible to reach a Reynolds number up to $3.5X10^7$ 1/m, but a lot of nitrogen and oxygen solids could appear in many locations. It is now possible to certify that the best settings to execute run test are T = 673 K and P = 40 bars. We know that using T=673 K and P=40 bars allow us to run simulations with good Reynolds numbers and stay over the condensation limit, so we will keep these two parameters to determine the flow quality in the test section.

C. Flow Quality in the Test Section

From the known flow parameters, we have studied temperature and condensation limits for the Ludwieg Tube. We now will study the flow quality, which will let us know the size of the usable volume in the test section. Firstly, we have to focus on how the streamlines, wince we need parallel streamlines in the test section in order to good results, and also to be able to put profiles or models in the Ludwieg Tube. All the simulations we have run gave us the same results presented in Fig. 18. Notice that the flow is steady and parallel. If we focus between 2.8m and 3.6m, which is the most interesting part for our study, we see that streamlines are almost parallel to the walls. We cam now analyze the flow in the test section more precisely.

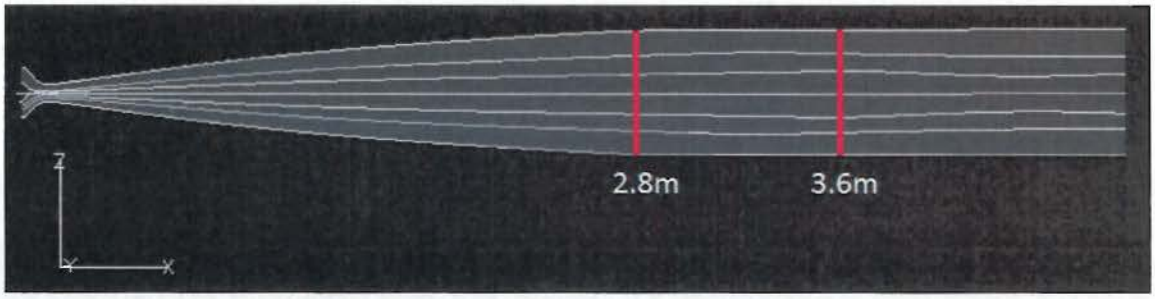

Figure 18: Streamlines in the Ludwieg Tube, plan (0;X;Z).

Flow in the test section

We have analyzed the test section from distances between 2.6m to 3.8m, in order to have a large number of values and be able to see the evolution of parameters in the flow. One of the most interesting parameters to analyze in the test section is pressure; we need to have a constant pressure evolution in the test section, which implies a constant pressure on cutting planes (Y; Z). Figure 19 shows the pressure from a cross-section at (2.7; 0; 0) to (3.8; 0; 0). We can see clearly that between 2.7m and 2.8m we have a transformation of the pressure distribution in the flow. At

2.7m pressure evolves between 1494 Pa and 2640 Pa and is not homogeneously distributed. On the contrary at 2.8m, we notice the pressure is constant around 2370 Pa. Then to 3.8m the pressure reduces steadily in the middle of the Ludwieg Tube, and we see that the area where the pressure is constant reduces from 2.8m.

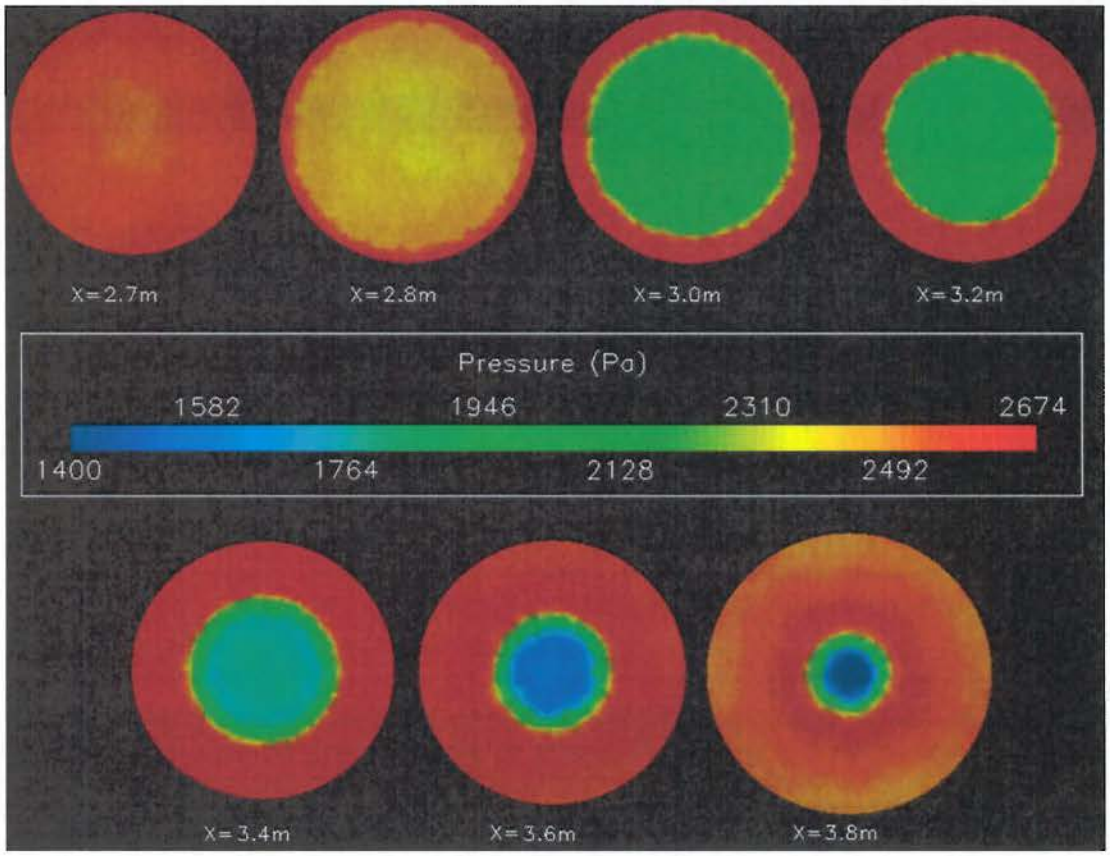

Figure 19: Pressure evolution in the test section from X=2.7m to X=3.8m.

To analyze pressure more precisely, we have made two dimensional plots of pressure. On the curves we notice an evolution in the pressure, and we have a stable pressure zone which starts at 2.7m to 3.6m. We also see that the size of this zone reduces; we have analyzed each cross-section shown in Figure 19, and the results are shown in Figures 20 through 22.

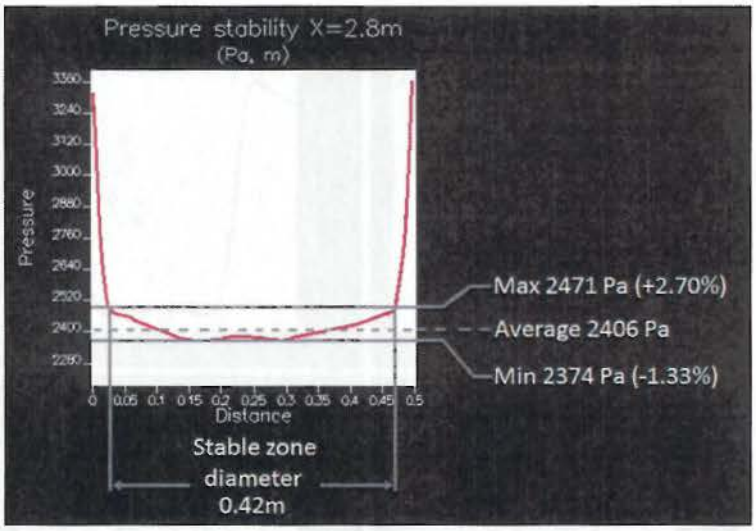

Figure 20: Example of pressure stability analyst for X=2.8m

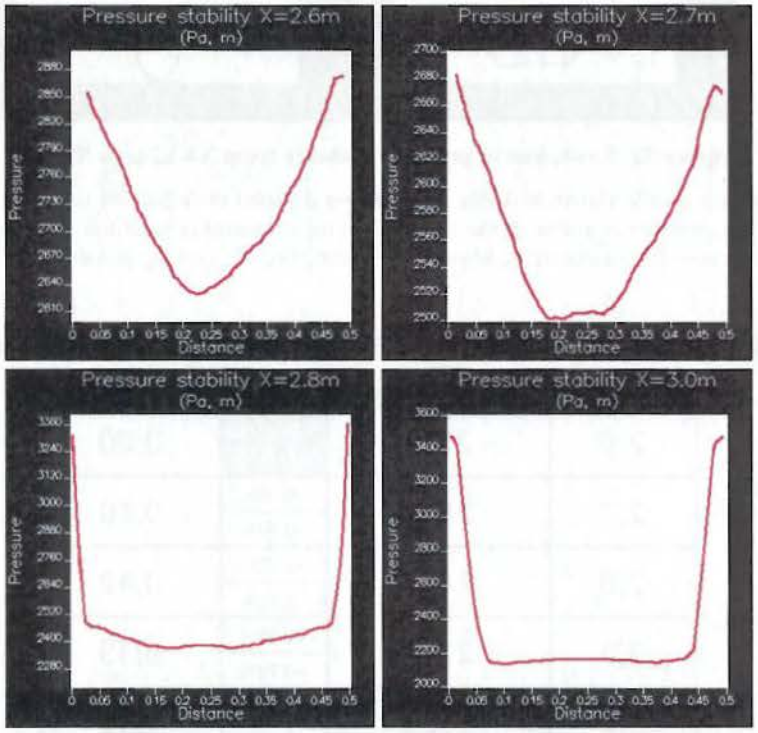

Figure 21: Evolution of pressure stability from X=2.6m to X=3.0m

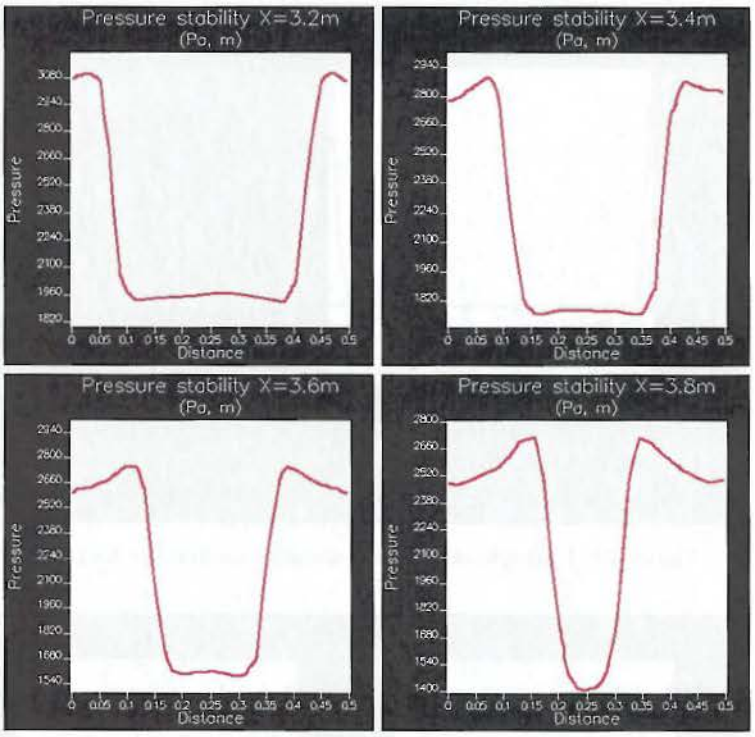

Figure 22: Evolution of pressure stability from X=3.2m to X=3.8m.

We obtained the summary results shown in Table 5, where we decided to define the test zone from X=2.8 to X=3.6. Indeed, before 2.8m the pressure is stable in the section but the diameter is too little to be used, we have the same problem after 3.6m because the diameter is fewer than 13cm. For all cutting planes, stability is always between +2.70% and -1.33%.

Table 5: Analysis of different curves for pressure stability in the test section

distance X (m)	Average pressure (Pa)	Stability	stable zone Ø (m)
2,6	2738		0,00
2,7	2504	+0,08%	0,10
		-0,16%	
2,8	2406	+2,70%	0,42
		-1,33%	
3,0	2153	+0,79%	0,35
		-0,79%	
3,2	1953	+0,87%	0,30
		-1,33%	
3,4	1768	+0,68%	0,21
		-0,79%	
3,6	1603	+0,62%	0,13
		-0,81%	
3,8	1425	+1,75%	0,05
		-0,70%	

Now that we have defined the test zone, we will focus on the Mach variation in this area. In the test section in the middle of the Ludwieg Tube the Mach number evolves from 5.95 to 6.33, as shown in Fig. 23. We have shown iso-

surfaces of Mach number colored by pressure, where we chose a Mach 5.95 iso-surface to see the general form of the useful area of test section, which is a truncated cone presented in the Fig. 23.

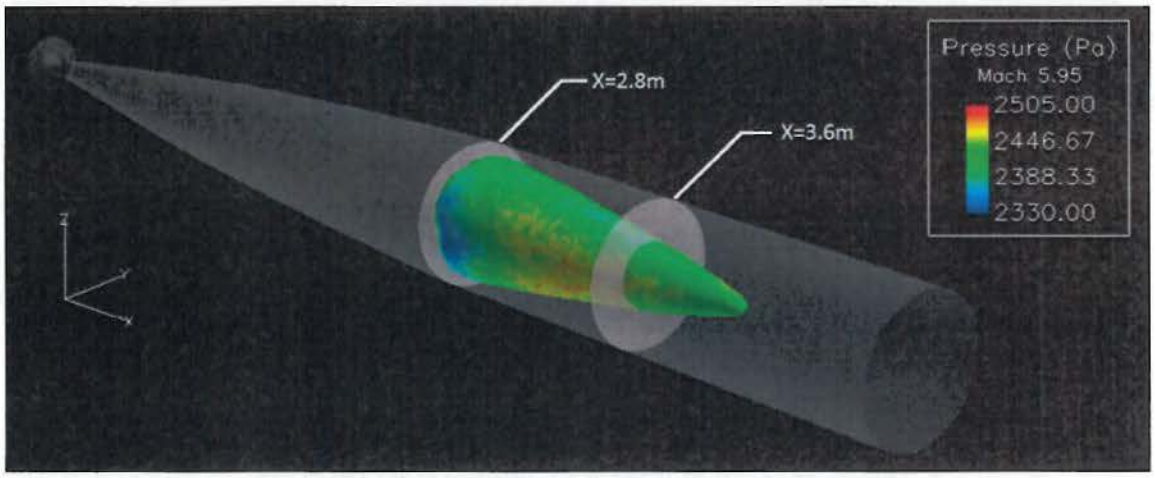

Figure 23: 3D view of the truncated cone work in the test section.

Indeed, the part of the cone over 3.6m cannot be used, because of its small size, but we can put a model or a profile in the rest of the cone to run simulations from at a nominal Mach number of 6.0. Models size can range from 0.42m to 0.13m. With the two dimensional plot tool of FieldView, we have analyzed the Mach number evolution between X=2.6m and X=3.8m and the result is the curve drawn in Fig. 24, which is almost a straight whose function is:

$$M(d) = 0.489d + 4.579$$

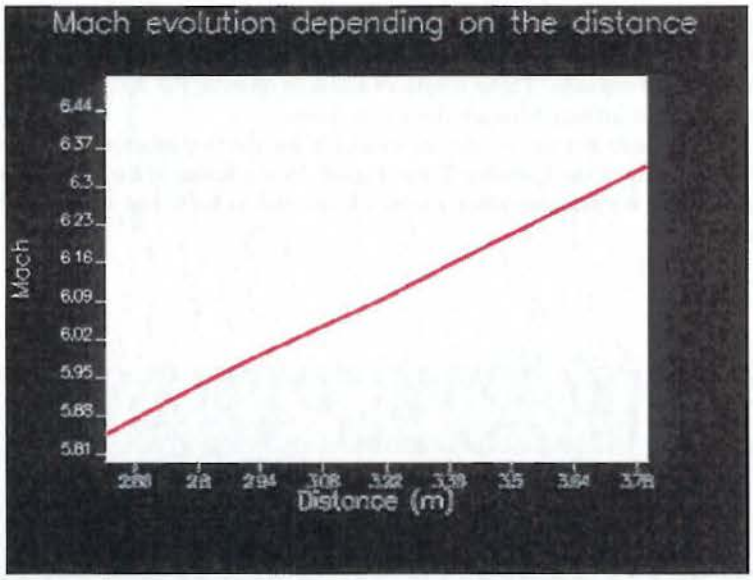

Figure 24: Mach evolution depending on the distance in the test section.

With this equation it is possible to predict the distance in the test section at which we must put a profile depending on the Mach number desired in a certain region. We notice the highest Mach zone has the shape of a cone, which is due to the Mach cone formed on the walls when the flow leaves the nozzle. We can measure the angle between the wall and the shock wave, as shown on Fig. 25.

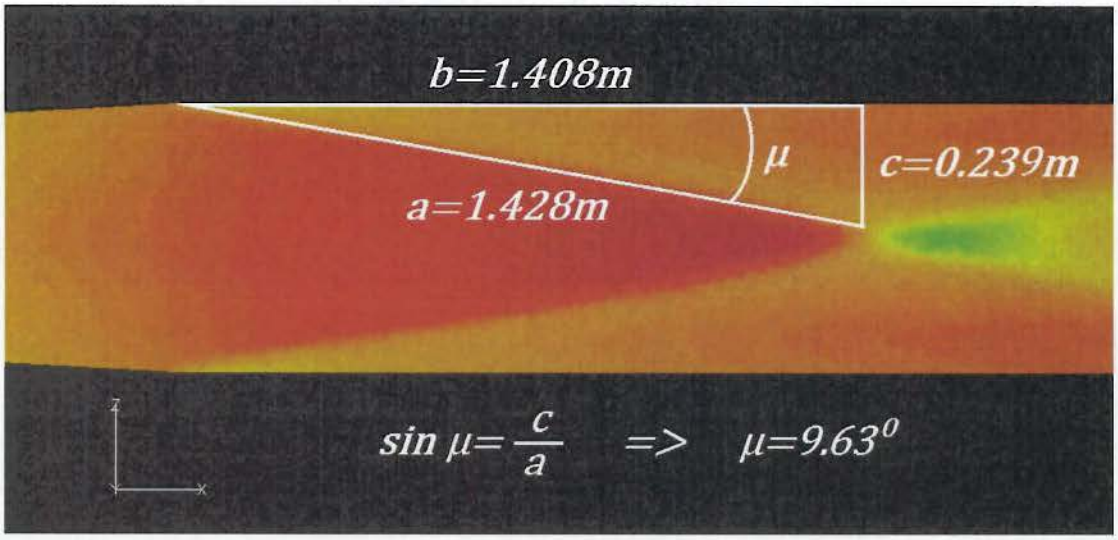

Figure 25: Analysis of Mach cone formed in the test section.

We can also calculate the angle with the Mach angle formula:

$$\mu = \sin^{-1}(1/M)$$

The calculation gives μ=9.59° at Mach 6, which matches very closely to the simulation results.

Flow at the Observation Window

This last section focuses on the observation windows and characteristics of the flow which will be possible to see and study with a camera. The three observation windows are 0.26m in diameter and positioned at 3.172m, one on the top, and one on each side of the tube. These windows allow to observe the flow from X=3.042m to 3.302m, and we need to know the flow characteristics between these two points.

We will focus on the right side but our results are available for the two other windows as well. We see that the window is in the hypersonic part of the Ludwieg Tube. Figure 26 is a zoom of the window with more details about the Mach number at this level. We see that Mach evolves from 6.06 to 6.19, and we know that we can put profiles measuring up to 0.25m.

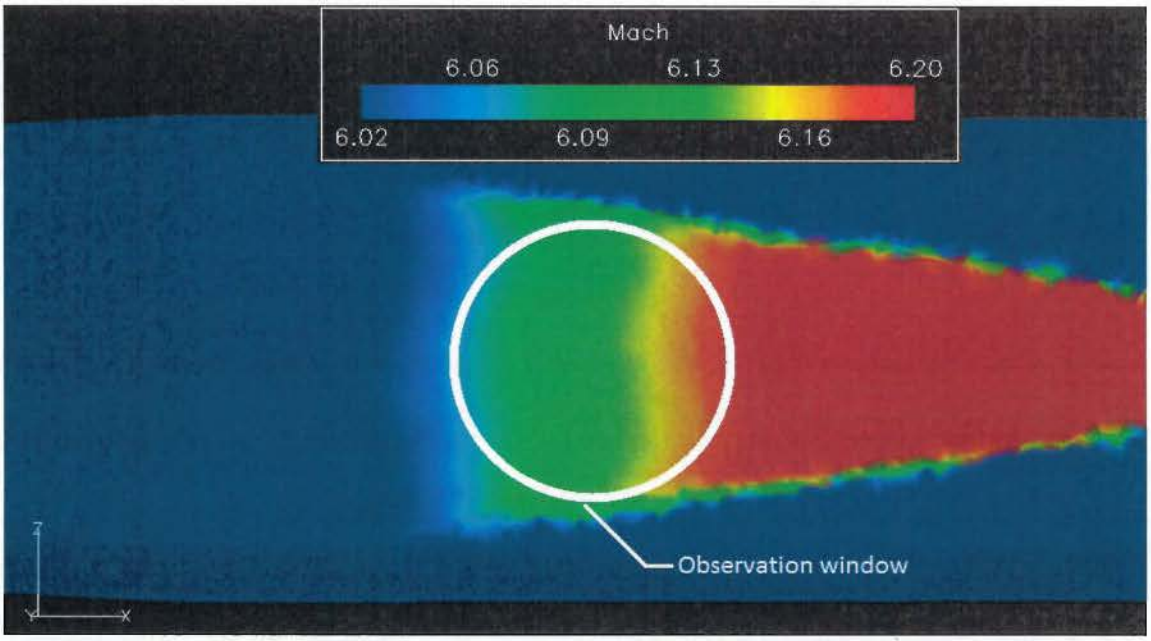

Figure 26: Zoom on the observation window, notice Mach 6.06 to 6.19.

Through observation windows we will be able to observe profiles and models in the hypersonic flow. With the increase of the quality of the new technology, like digital cameras and the computer, we are now able to use direct pictures of the flow to find the density field. This is possible because the light is deflected through the flow when density changes. This technology, named Background-Oriented Schlieren (BOS), has been studied at USAFA during the Summer of 2011 by Captain Laurent Savio from the French Air Force during his internship. Future scientists and USAFA students will be able to use this technology on the Ludwieg Tube.

IV. Conclusions

Among the equations which are available to resolve fluid dynamics problem, we used the Euler equations to study the flow field in the Mach 6 Ludwieg Tube wind tunnel. Using CFD, we were able to choose a grid which showed the flow in the test section of the tunnel.

Before running any calculations, it was important to find the right boundary conditions. If the charge tube pressure and temperature are allowed to vary, the Mach number in the charge tube (at the valve) and the outflow pressure have to be set. We found that M = 0 gave us the best results. The vacuum tank can reduce the outflow pressure conclude that a charge tube pressure P = 40 bars and a charge tube temperature T = 673 K are to 100 Pa; we choose 1000 Pa in the wake of some difficulties to complete some calculations with a lower pressure.

Thanks to about thirty calculations we have found a useful range of the Ludwieg Tube without taking the condensation into account. This latest constraint has reduced this range and finally we have the best settings to maintain the flow in gaseous phase.

In order to anticipate future works, we have also determined the dimensions of the test zone, and have demonstrated the pressure stability inside of it. This stability is a guaranty of the quality allowing a constant flow in the test section. Indeed, the Ludwieg Tube is designed to reach Mach 6; our simulations have shown that we reach Mach 5.95 to 6.33 in a 0.80 meter-long test zone. We can use models up to 0.40 meters in the test section. We have also determined the flow parameters in the observation windows, making it possible to use Background-Oriented Schlieren technology.

During our project we ran calculations using the new operating system and software, analyzed results and defined necessary equations and useful computational mesh. We found boundary conditions which allowed us to determine the best test section of the Ludwieg Tube. We sized the test section and calculated its performance. By working on these different parameters and values, making choices according to our results we have reached our goal which was to evaluate and accurate computational modeling of the Ludwieg Tube.

Acknowledgments

We want to thank Captain Laurent Savio for his help and his confidence in our project since the beginning. We also thank Major Jerome D'Oliveira, French Liaison Officer at USAFA, for his work in setting up our exchange program, Mr. Robert Decker of the Modeling & Simulation Research Center (MSRC) for making the grids, Mr. Rudolf Mueller-Eigner of Hyperschall und Stromungstechnik GmbH for supplying the CAD file, Mr. Mehdi Ghoreyshi for his advice, Mr. Malte Estorf of the Technical University at Braunschweig Institute for Fluid Mechanics, the MSRC at USAFA and Mr. Joshua Durbin for logistics. We also appreciate the support of the MSRC at USAFA for supplying the computational resources used in this work.

References

[1]Cummings, R.M. and Thomas McLaughlin, T.E., "Hypersonic Ludwieg Tube Design and Future Usage at the US Air Force Academy," AIAA Paper 2012-0734, Jan. 2012

[2] H. Ludwieg, "Der Rohrwindkanal," *Z.F. Flugwiss.*, Vol. 3, No. 7, 1955, pp. 206-216.

[3] G. Koppenwallner, "Hypersonic Flow Simulation in Ludwieg Tube," Int. Symposium on Recent Advances in Experimental Fluid Dynamics, IIT Kanpur India 2000.

[4] M. Estorf, T. Wolf, and R. Radespiel, "Experimental and Numerical Investigations on the Operation of the Hypersonic Ludwieg Tube Braunschweig," Fifth European Symposium on Aerothermodynamics for Space Vehicles, Cologne Germany, 2004.

[5] G. Koppenwallner and R. Müller-Eigner, "Detailed Design of Ma = 6 Ludwieg Tube Wind Tunnel for the USAF Academy," HST-TN-3-2011, September 2011.

[6]Strang, W. Z., Tomaro, R. F., and Grismer, M. J., "The Defining Methods of Cobalt: A Parallel, Implicit, Unstructured Euler/Navier-Stokes Flow Slover," AIAA Paper 1990-0786, Jan. 1999.

[7]Gottlieb, J. J. and Groth, C. P. T., "Assessment of Riemann Solvers for Unsteady One-Dimensional Inviscid Flows of Perfect Gasses," *Journal of Computation Physics*, Vol. 78, No. 2, Jan. 1998, pp. 437–458.

[8]Tomaro, R. F., Strang, W. Z., and Sankar, L. N., "An Implicit Algorithm for Solving Time Dependent Flows on Unstructured Grids," AIAA Paper 1997-0333, Jan. 1997.

[9]Koppenwallner, G. (HTG Hypersonic-Technology-Göttingen) ; Condensation analysis for air operated Mach 6 Ludwieg Tube wind tunnel ; Study report for US Air Force Academy Colorado (1-30-2010)